Extracting Microphysical Impacts in Large-Eddy Simulations of Shallow Convection

WOJCIECH W. GRABOWSKI

National Center for Atmospheric Research,* Boulder, Colorado

ABSTRACT

A simple methodology is proposed to extract impacts of cloud microphysics on macrophysical cloud-field properties in large-eddy simulations of shallow convection. These impacts are typically difficult to assess because of natural variability of the simulated cloud field. The idea is to use two sets of thermodynamic variables driven by different microphysical schemes or by a single scheme with different parameters as applied here. The first set is coupled to the dynamics as in the standard model, and the second set is applied diagnostically—that is, driven by the flow but without the feedback on the flow dynamics. Having the two schemes operating in the same flow pattern allows for extracting the impact with high confidence. For illustration, the method is applied to simulations of precipitating shallow convection applying a simple bulk representation of warm-rain processes. Because of natural variability, the traditional approach provides an uncertain estimate of the impact of cloud droplet concentration on the mean cloud-field rainfall even with an ensemble of simulations. In contrast, the impact is well constrained while applying the new methodology. The method can even detect minuscule changes of the mean cloud cover and liquid water path despite their large temporal fluctuations and different evolutions within the ensemble.

1. Motivation

Assessing impacts of cloud microphysics on macrophysical properties of simulated shallow convective cloud fields (e.g., the cloud cover, mean precipitation, liquid water path) is difficult. This is because the cloud cover is typically small (say, 10%), clouds evolve rapidly through their lifestyle, and the cloud field differs significantly at various moments of the simulation. Arguably, all these are related to the natural variability of shallow convection. As a result, many measures of the cloud-field characteristics (such as profiles of domain-averaged cloud variables and surface precipitation) show large departures from time averages; see Figs. 2 and 4 in Xue and Feingold (2006), Figs. 2 and 4 in Stevens and Seifert (2008), Fig. 3 in vanZanten et al. (2011), Figs. 9–12 in Wyszogrodzki et al. (2013), and Fig. 4 in Franklin (2014) for specific examples. Extracting the impact of cloud microphysics with high

confidence requires substantial effort—for instance, applying an ensemble of simulations, using large horizontal domains or extended simulations, all aimed at limiting the impact on natural variability.

We propose here a novel methodology to provide a confident assessment of the effect of cloud microphysics in large-eddy simulations of shallow convective cloud fields. The approach has some similarities to the method applied by Kooperman et al. (2012) to improve estimates of the global aerosol indirect effects. To reduce the impact of natural variability, Kooperman et al. nudged GCM simulations with different aerosol emissions toward the same meteorological conditions and obtained statistically significant estimates of aerosol indirect effects in considerably shorter simulations. A similar method is proposed here. We apply two microphysical schemes in the same dynamical setup; that is, one scheme drives the dynamics and the other one just tags along the flow field simulated by the model. In other words, both schemes are operating in a realistic (3D, time evolving, etc.) flow field. Such a methodology is a significant improvement over the kinematic (prescribed flow) strategy used in the past to compare simulations with various microphysical schemes (e.g., Szumowski et al. 1998; Morrison and Grabowski 2007; Shipway and Hill 2012).

2. The methodology

The proposed method is embarrassingly simple. The main idea is to use two sets of thermodynamics variables, each set affected by a different microphysics scheme or by the same scheme featuring different sets of scheme parameters. One set drives the dynamics as in the standard model (the prognostic scheme) and the other one tags along (piggybacks) the simulated flow field (the diagnostic scheme). The model needs to be modified to allow two sets of thermodynamics variables—that is, the potential temperature and water vapor mixing ratio as well as all variables used to describe cloud and precipitation particles. The fields from the prognostic set are used in the buoyancy, and the other set is solved as in the kinematic model (i.e., without affecting the dynamics). If additional processes modifying thermodynamic variables are included in the model physics (e.g., surface fluxes, radiative transfer, prescribed large-scale advective tendencies), they need to be calculated independently for each set. After completing the first simulation, the second simulation can be run with the prognostic and diagnostic sets switched so the previously diagnostic set becomes the prognostic one, and vice versa. Comparing the two simulations hints at the impact (or lack thereof) of the cloud microphysics on the dynamics as discussed later in the paper. At the end, the approach results in two simulations, each featuring two sets of thermodynamic variables: one prognostic and one diagnostic (i.e., four sets of thermodynamic variables altogether). Microphysics parameterizations of various complexities can be considered. For instance, a parameterization that includes warm-rain processes only can be contrasted with a scheme permitting ice processes. This allows assessing the role of ice processes and separates a purely thermodynamic impact (e.g., more water vapor available for particle growth below freezing with ice microphysics) from the dynamical effect (e.g., presence of deeper clouds because of the increased latent heating and larger buoyancy for the ice case).

We apply the proposed methodology to the shallow-precipitating-convection case based on the Barbados Oceanographic and Meteorological Experiment (BOMEX) model intercomparison setup (Siebesma et al. 2003, hereafter S03). To document fidelity of the approach, we consider the impact of prescribed cloud droplet concentration on macroscopic cloud-field properties and contrast simulations with a relatively small difference in the prescribed concentrations.

3. The model and modeling setup

The model used in this study is a simplified serial version of the 3D nonhydrostatic anelastic Eulerian–semi-Lagrangian

(EULAG) model (see http://www.mmm.ucar.edu/eulag/) sometimes referred to as the babyEULAG. As does its parent, babyEULAG applies a nonoscillatory forward-in-time integration scheme based on the multidimensional positive definite advection transport algorithm (MPDATA; e.g., Smolarkiewicz 2006) and uses an elliptic pressure solver for the anelastic dynamics [see Prusa et al. (2008) for a review and comprehensive list of references]. The babyEULAG does not have any subgrid-scale turbulence scheme but it employs the implicit large-eddy simulation (ILES) approach (Margolin et al. 2006; Grinstein et al. 2007). Such an approach exploits the properties of high-resolution nonoscillatory finite-volume methods; see Waite and Smolarkiewicz (2008) for an ILES application to the large-Reynolds-number vortex-pair dynamics in a strongly stratified fluid.

The cloud microphysics scheme applied in simulations described here is the single-moment scheme documented in Grabowski (1998, hereafter G98) with centered-in-time integration for the saturation adjustment and forward-Euler (uncentered) scheme for precipitation processes; see Grabowski and Smolarkiewicz [1996, cf. Eqs. (8) and (9) therein]. Although the scheme does include a simple representation of ice process, these are irrelevant for the warm (ice free) simulations considered here. The conversion of cloud water into drizzle/rain (the autoconversion) is represented based on the formulation proposed by Berry (1968) as applied by Simpson and Wiggert (1969, their section 3). The warm-rain autoconversion depends on the local values of the cloud water mixing ratio, cloud droplet concentration, and the relative dispersion of the cloud droplet spectrum, with the latter two required to be specified [cf. Eq. (8) in G98]. We consider simulations that apply two droplet concentrations, $N = 70$ and $N = 100 \, \text{cm}^{-3}$, and assume the relative spectral dispersion of 0.3. Such a formulation leads to the autoconversion term of about 2×10^{-9}, 10^{-6}, and $3 \times 10^{-4} \, \text{kg} \, \text{kg}^{-1} \, \text{s}^{-1}$ for cloud water mixing ratios of 0.1, 1, and $10 \, \text{g} \, \text{kg}^{-1}$, respectively, for $N = 70 \, \text{cm}^{-3}$. For $N = 100 \, \text{cm}^{-3}$, the autoconversion is reduced by about 30% for cloud water of 0.1 and $1 \, \text{g} \, \text{kg}^{-1}$ and by about 7% for $10 \, \text{g} \, \text{kg}^{-1}$. It follows that one should expect some reduction of precipitation in the higher-droplet-concentration case. We stress that the particular autoconversion parameterization is applied here only to document the fidelity of the proposed methodology and not to study the impact of the parameterization on the rain from shallow convection. For the latter, perhaps a more up-to-date formulation should be used—for instance, as in Kogan (2013).

A simulation in which the thermodynamic set with $N = 70 \, \text{cm}^{-3}$ drives the dynamics and $N = 100 \, \text{cm}^{-3}$ set tags along will be referred to as the D70/P100 simulation
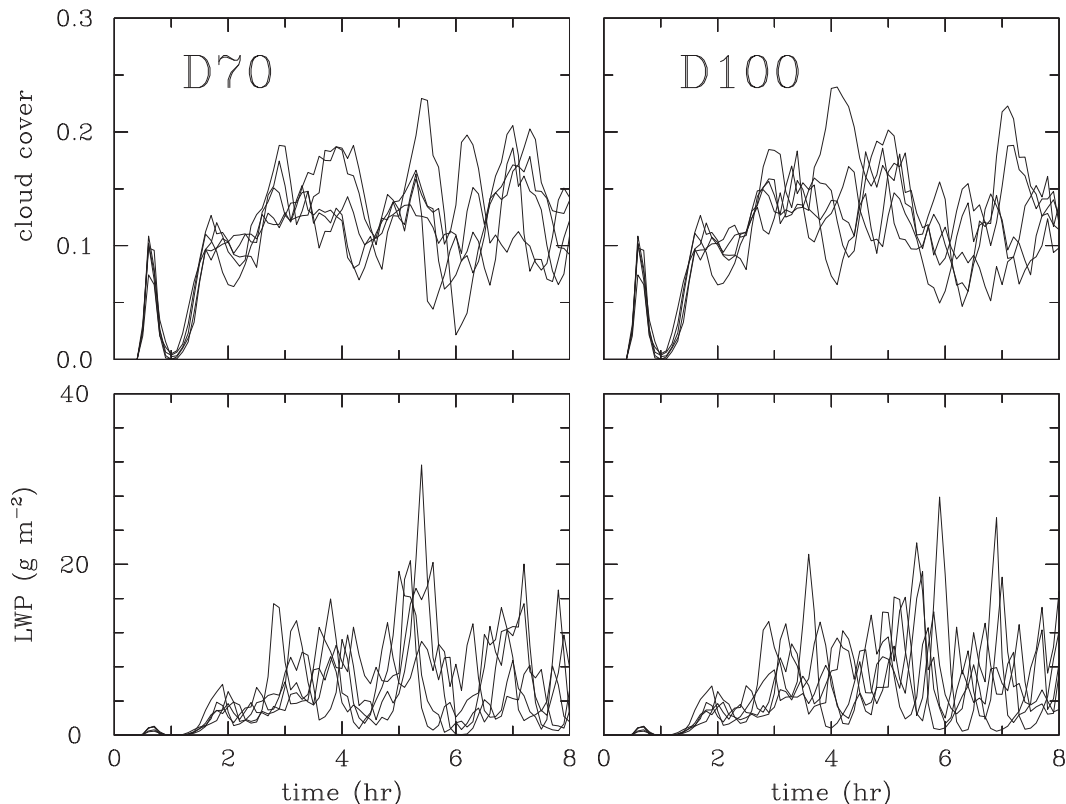
FIG. 1. Evolution of (top) the cloud cover and (bottom) LWP for five-member ensembles of (left) D70 and (right) D100 of BOMEX simulations.

("D" for "dynamic" and "P" for "piggybacking"). A complementary simulation with the thermodynamic schemes switched will be referred to as D100/P70. The two simulations result in four sets of thermodynamic variables: namely, D70, D100, P70, and P100. Five sets of simulations are performed, each set containing two simulations (i.e., one D70/P100 and one D100/P70). The only difference for each set is a different draw of random numbers generated when imposing the initial temperature and moisture perturbations as described in S03. D70 and D100 results can be compared as in a traditional ensemble methodology. Analyzing results for ensemble member pairs D70–P100 and D100–P70 allows for extracting microphysical impacts as documented in the following discussion.

The model setup is exactly as described in S03 except that the simulations are run for 8 h instead of 6 h and precipitation processes are allowed as in Wyszogrodzki et al. (2013) and Grabowski et al. (2014). The model time step is 2.5 s. Snapshots of 3D model fields are saved every 6 min. In addition, 2D surface rain rate is saved every minute as an average from the previous minute. The two datasets are used in the analysis presented here.

4. Results

As already explained, assessing the impact of a relatively small change in the cloud microphysics is difficult and uncertain because of the natural variability. This is illustrated in Fig. 1, which shows evolutions of the cloud cover (the fraction of columns with the cloud water somewhere within the column) and the liquid (cloud and precipitation) water path (LWP) for D70 and D100 sets. In agreement with results shown in S03 (cf. Fig. 2 therein), model spinup lasts for about 90 min with solutions following each other. After the spinup, the solutions diverge and follow different paths in the phase space that represent different realizations of the system evolution due to inherently nonlinear system dynamics.

Fluctuations of the cloud field have strong impacts on the surface precipitation. This is documented in Fig. 2, which shows evolutions of the surface rain rate and total rain accumulation for selected members of the D70 and D100 ensembles. As the figure shows, significant mean surface precipitation occurs in sporadic events, most likely associated with the presence of the deepest clouds. Total accumulations at the end of simulations (i.e., at 8 h) differ significantly between the ensemble members. As
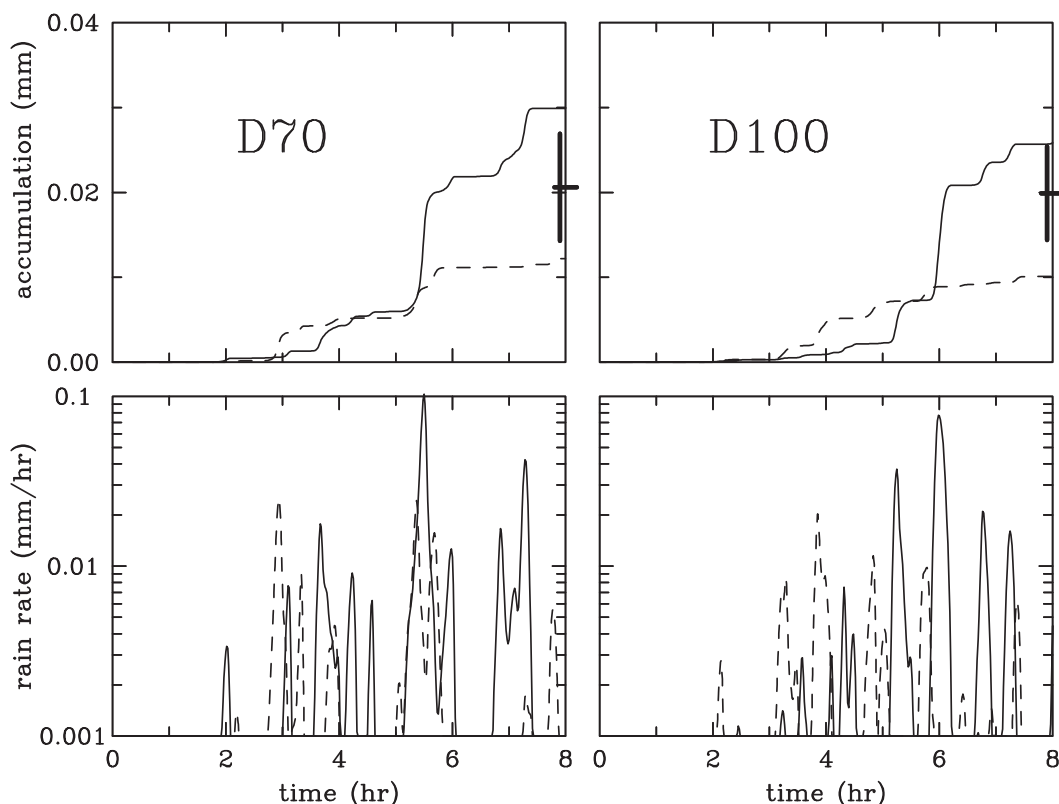
FIG. 2. Evolution of (bottom) the horizontally averaged surface precipitation rate and (top) the surface rain accumulation for the two ensemble members that show the largest (solid lines) and the smallest (dashed lines) surface rain accumulation at 8 h for (left) D70 and (right) D100 simulations. Thick lines in the top panels show the ensemble mean and the range (the mean plus and minus one standard deviation among the members) of the accumulation at 8 h.

shown in Table 1, the mean values for D70 and D100 are 2.06×10^{-2} and 1.99×10^{-2} mm, with the standard deviation between ensemble members of 0.63×10^{-2} and 0.55×10^{-2} mm. Since the difference between D70 and D100 ensemble is much smaller than the standard deviation within each ensemble, the difference can be argued as uncertain and statistically insignificant. A larger ensemble or longer simulations would be needed to obtain statistically significant results.

Figure 3, in the format of Fig. 2, shows results obtained applying the methodology advocated in this paper for two randomly selected pairs of D70/P100 and D100/P70 ensemble members. Although cloud field evolutions are different in the two simulations, the diagnostic scheme (P100 and P70 in the left and right panels, respectively) allows a confident evaluation of the autoconversion impact. As the figure shows, the same evolution of the cloud field and thus the same surface precipitation events result in systematic differences in the surface rate and total accumulation—larger for the lower-droplet-concentration simulations. As documented in Table 1, the increase of the surface rain accumulation is practically

the same in both ensembles: about 0.4×10^{-2} mm with the standard deviation of around 20% of this value.

Comparing results from the two ensembles (i.e., D70/P100 and D100/P70) hints at an insignificant impact of the cloud microphysics on the cloud dynamics. If there were a strong impact (e.g., one ensemble featured significantly deeper clouds), then the difference between

TABLE 1. Domain-averaged surface rain accumulation (10^{-2} mm) for 8 h of BOMEX simulations. St. dev. refers to the standard deviation of (third column) the mean and (fourth column) the mean D − P difference among ensemble members. The data come from two ensembles. Each member of the ensemble includes one set of thermodynamic variables that drives the flow (D70 and D100) and another set that is piggybacking the simulation (P100 for D70 and P70 for D100). The impact is assessed by comparing the D70–P100 and D100–P70 pairs.

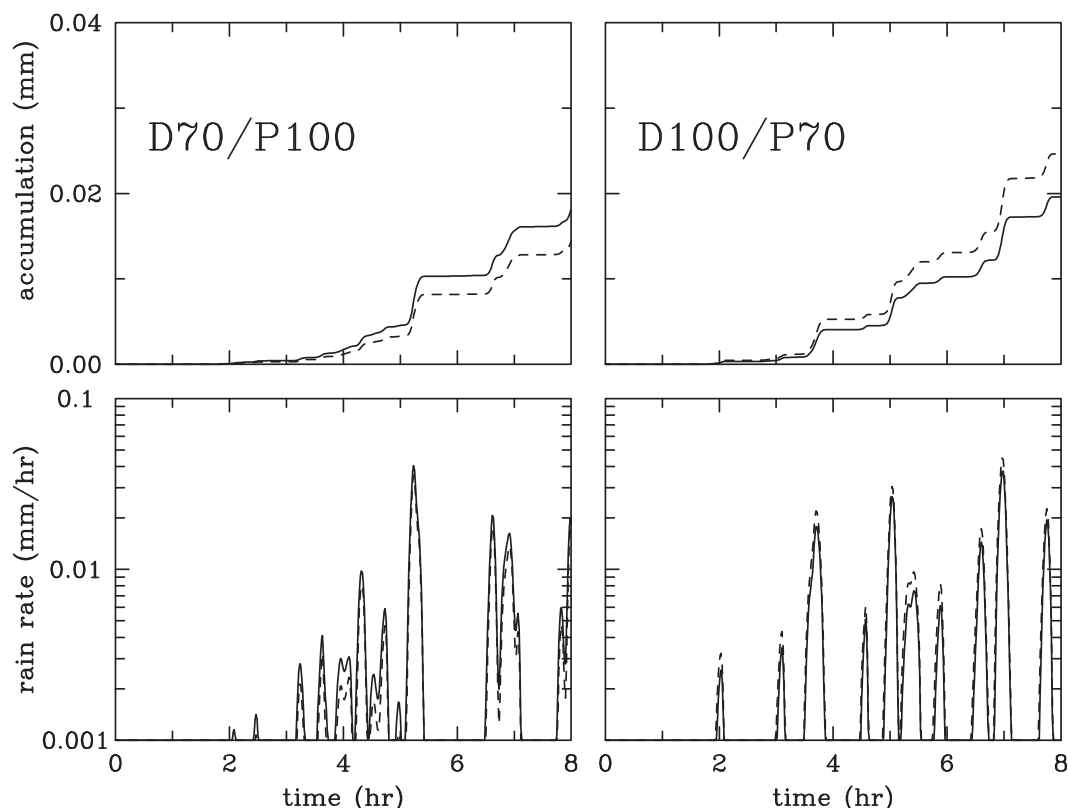| Set	Accumulation for each member	Ensemble: mean, st. dev.	D − P: mean, st. dev.
D70	2.54, 1.72, 2.99, 1.81, 1.22	2.06, 0.63	0.41, 0.08
D100	1.01, 1.97, 1.96, 2.58, 2.43	1.99, 0.55	−0.43, 0.07
P100	2.06, 1.33, 2.48, 1.44, 0.94	1.65, 0.55	—
P70	1.32, 2.38, 2.46, 3.04, 2.91	2.42, 0.60	—

FIG. 3. As in Fig. 2, but for single ensemble members of the D70 and D100 simulations (solid lines) and corresponding results for P100 and P70 (dashed lines) for (left) D70/P100 and (right) D100/P70.

the ensembles and especially the change from D to P (i.e., the reduction from D70 to P100 and the increase from D100 to P70) would likely be different. Because the reduction (increase) of the total accumulation between D70 and P100 (D100 and P70) is practically the same in both ensembles, the dynamics of individual clouds seems to be only weakly affected by the feedback from the microphysics. In other words, the difference between the two ensembles comes mostly from different microphysics (i.e., more efficient conversion of cloud water into rain) and not likely from the cloud dynamics (e.g., deeper clouds for one of the ensembles). This is

supported by the distributions of cloud-top heights that show statistically insignificant differences between D70 and D100 sets (not shown).

To further illustrate the fidelity of the method, we consider changes of the cloud cover and LWP. As illustrated in Fig. 1, addressing the changes using D simulations alone is impossible. Table 2, in the format of Table 1, shows that the D ensemble-mean cloud cover and LWP increase (from 0.129 to 0.131 and from 6.27 to 6.52 g m^{-2}, respectively) with the increase of the droplet concentration. Arguably, this is consistent with the second indirect aerosol effect—that is, less efficient removal of cloud

TABLE 2. As in Table 1, but for the hour 2–8 averages of the cloud cover and domain-averaged LWP (g m^{-2}).

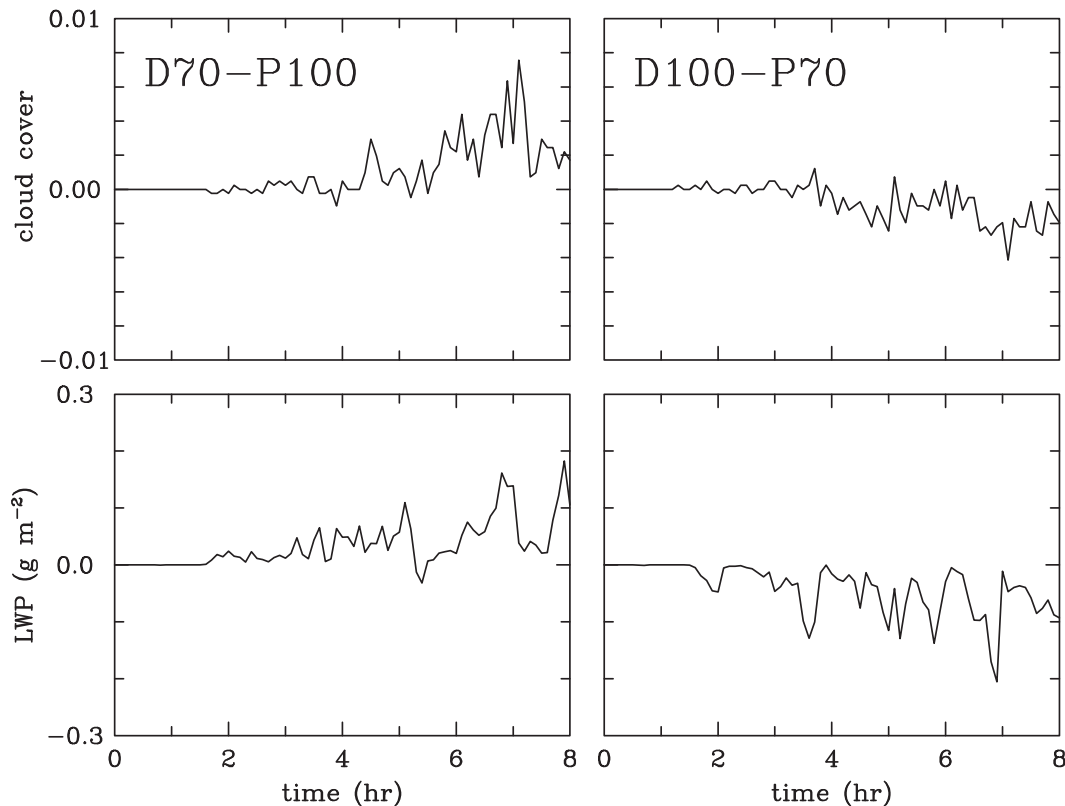| Set	6-h mean for each member	Ensemble: mean, st. dev.	D − P: mean, st. dev.
Cloud cover			
D70	0.126, 0.126, 0.129, 0.131, 0.135	0.129, 0.003	0.001, 0.0004
D100	0.146, 0.126, 0.120, 0.133, 0.130	0.131, 0.009	−0.001, 0
P100	0.125, 0.125, 0.128, 0.129, 0.133	0.128, 0.003	—
P70	0.147, 0.127, 0.121, 0.134, 0.131	0.132, 0.008	—
Mean LWP			
D70	6.49, 6.16, 6.82, 6.32, 5.59	6.27, 0.41	0.05, 0.01
D100	6.05, 6.29, 7.06, 6.39, 6.81	6.52, 0.37	−0.05, 0.01
P100	6.45, 6.11, 6.76, 6.28, 5.54	6.22, 0.41	—
P70	6.10, 6.34, 7.12, 6.44, 6.87	6.57, 0.37	—

FIG. 4. Evolutions of (top) the cloud cover and (bottom) LWP differences between (left) D70 and P100 and (right) D100 and P70 for ensemble members as in Fig. 3.

water for weaker precipitating clouds leading to more liquid water in the atmosphere. However, standard deviations among ensemble members are larger than the difference and thus the difference is not statistically significant. Comparing D and P sets, however, provides a different outcome, with the cloud cover and LWP reduced when droplet concentration is higher, by 0.001 and 0.05 g m^{-2} for the cloud cover and LWP, respectively. This is further illustrated in Fig. 4, which shows evolutions of the cloud cover and LWP difference between D and P sets (rather than evolutions of both D and P as in Fig. 3) because the differences are extremely small (cf. the units on the vertical axes of Figs. 1 and 4). Table 2 shows that the differences illustrated in Fig. 4 apply to all members of the ensemble; that is, the averaged differences for D70 − P100 are positive and for D100 − P70 are negative. These differences are of the opposite sign when compared to the D ensemble means and seem inconsistent with the second indirect aerosol effect. However, an explanation is possible and it likely involves fundamental features of the bulk warm-rain microphysics that involve immediate evaporation of cloud condensate in subsaturated conditions and finite-time evaporation of rain. In other words, having more rain in a bulk warm-rain scheme provides

a delay in the liquid water (cloud plus rain) evaporation. The time-averaged differences (see Table 2) are minuscule—roughly at the 1% level (e.g., 0.001 for 0.13 for the cloud cover and 0.05 for 6 g m^{-2} for LWP). However, they are statistically significant based on the values of ensemble standard deviations.

5. Conclusions and outlook

We propose a simple methodology to improve the understanding of the effects of cloud microphysics on cloud simulations. The idea is to apply one set of thermodynamic variables (the temperature, water vapor mixing ratio, and cloud and precipitation variables) as usually applied in a cloud model (i.e., coupled to the flow dynamics through the buoyancy term) and then drive the second set in the kinematic manner—that is, responding to the flow evolution but not affecting the flow. Simulations presented here document the potential of the new approach in large-eddy simulations of shallow precipitating convection. We also argue that reversing the way schemes are applied (i.e., switching the previously dynamic set of variables into the kinematic mode and vice versa) allows for estimating the impact of the

microphysics on the dynamics. However, such an estimate is uncertain because it is affected by the natural variability between the two simulations.

We are currently applying the same methodology in simulations of deep convection to study the problem of convective invigoration in polluted environments (Grabowski 2014, manuscript submitted to *J. Atmos. Sci.*). The piggybacking methodology allows an unprecedented look at the effects of the suppressed warm-rain processes and enhanced ice processes in polluted deep convection. We are also aware of an ongoing effort within the U.S. Department of Energy Atmospheric System Research Program to apply the piggybacking methodology in order to provide improved evaluations of microphysical schemes in cloud simulations (J. Fan et al. 2014, personal communication). We plan to apply the piggybacking methodology to the bin microphysics simulations targeting the impact of small-scale turbulence on warm-rain formation in shallow convection described in Wyszogrodzki et al. (2013) and in Grabowski et al. (2014). Finally, the same methodology can also be used to extract the impact of other parameterizations, such as the surface fluxes or radiation, in model simulations.

REFERENCES

Berry, E. X., 1968: Modification of the warm rain process. *Proc. First Conf. on Weather Modification,* Albany, NY, Amer. Meteor. Soc., 81–85.

Franklin, C. N., 2014: The effects of turbulent collision–coalescence on precipitation formation and precipitation-dynamical feedbacks in simulations of stratocumulus and shallow cumulus convection. *Atmos. Chem. Phys.,* **14,** 6557–6570, doi:10.5194/acp-14-6557-2014.

Grabowski, W. W., 1998: Toward cloud resolving modeling of large-scale tropical circulations: A simple cloud microphysics parameterization. *J. Atmos. Sci.,* **55,** 3283–3298, doi:10.1175/1520-0469(1998)055<3283:TCRMOL>2.0.CO;2.

——, and P. K. Smolarkiewicz, 1996: Two-time-level semi-Lagrangian modeling of precipitating clouds. *Mon. Wea. Rev.,* **124,** 487–497, doi:10.1175/1520-0493(1996)124<0487:TTLSLM>2.0.CO;2.

——, L.-P. Wang, and T. V. Prabha, 2014: Impacts of cloud and precipitation processes on maritime shallow convection as simulated by an LES model with bin microphysics. *Atmos. Chem. Phys. Discuss.,* **14,** 19 837–19 873, doi:10.5194/acpd-14-19837-2014.

Grinstein, F. F., L. G. Margolin, and W. J. Rider, 2007: *Implicit Large Eddy Simulation: Computing Turbulent Fluid Dynamics.* Cambridge University Press, 578 pp.

Kogan, Y., 2013: A cumulus cloud microphysics parameterization for cloud-resolving models. *J. Atmos. Sci.,* **70,** 1423–1436, doi:10.1175/JAS-D-12-0183.1.

Kooperman, G. J., M. S. Pritchard, S. J. Ghan, M. Wang, R. C. J. Somerville, and L. M. Russell, 2012: Constraining the influence of natural variability to improve estimates of global aerosol indirect effects in a nudged version of the Community Atmosphere Model 5. *J. Geophys. Res.,* **117,** D23204, doi:10.1029/2012JD018588.

Margolin, L. G., W. J. Rider, and F. F. Grinstein, 2006: Modeling turbulent flow with implicit les. *J. Turbul.,* **7,** doi:10.1080/14685240500331595.

Morrison, H., and W. W. Grabowski, 2007: Comparison of bulk and bin warm-rain microphysics models using a kinematic framework. *J. Atmos. Sci.,* **64,** 2839–2861, doi:10.1175/JAS3980.

Prusa, J. M., P. K. Smolarkiewicz, and A. A. Wyszogrodzki, 2008: EULAG, a computational model for multiscale flows. *Comput. Fluids,* **37,** 1193–1207, doi:10.1016/j.compfluid.2007.12.001.

Shipway, B. J., and A. A. Hill, 2012: Diagnosis of systematic differences between multiple parametrizations of warm rain microphysics using a kinematic framework. *Quart. J. Roy. Meteor. Soc.,* **138,** 2196–2211, doi:10.1002/qj.1913.

Siebesma, A. P., and Coauthors, 2003: A large eddy simulation intercomparison study of shallow cumulus convection. *J. Atmos. Sci.,* **60,** 1201–1219, doi:10.1175/1520-0469(2003)60<1201:ALESIS>2.0.CO;2.

Simpson, J., and V. Wiggert, 1969: Models of precipitating cumulus towers. *Mon. Wea. Rev.,* **97,** 471–489, doi:10.1175/1520-0493(1969)097<0471:MOPCT>2.3.CO;2.

Smolarkiewicz, P., 2006: Multidimensional positive definite advection transport algorithm: An overview. *Int. J. Numer. Methods Fluids,* **50,** 1123–1144, doi:10.1002/fld.1071.

Stevens, B., and A. Seifert, 2008: Understanding macrophysical outcomes of microphysical choices in simulations of shallow cumulus convection. *J. Meteor. Soc. Japan,* **86A,** 143–162.

Szumowski, M. J., W. W. Grabowski, and H. T. Ochs III, 1998: Simple two-dimensional kinematic framework designed to test warm rain microphysical models. *Atmos. Res.,* **45,** 299–326, doi:10.1016/S0169-8095(97)00082-3.

vanZanten, M. C., and Coauthors, 2011: Controls on precipitation and cloudiness in simulations of trade-wind cumulus as observed during RICO. *J. Adv. Model. Earth Syst.,* **3,** M06001, doi:10.1029/2011MS000056.

Waite, M. L., and P. K. Smolarkiewicz, 2008: Instability and breakdown of a vertical vortex pair in a strongly stratified fluid. *J. Fluid Mech.,* **606,** 239–273, doi:10.1017/S0022112008001912.

Wyszogrodzki, A. A., W. W. Grabowski, L.-P. Wang, and O. Ayala, 2013: Turbulent collision-coalescence in maritime shallow convection. *Atmos. Chem. Phys.,* **13,** 8471–8487, doi:10.5194/acp-13-8471-2013.

Xue, H., and G. Feingold, 2006: Large-eddy simulations of trade wind cumuli: Investigation of aerosol indirect effects. *J. Atmos. Sci.,* **63,** 1605–1622, doi:10.1175/JAS3706.1.